Propagation of firing rate by synchronization and coherence of firing pattern in a feed-forward multilayer neural network

Ming Yi*
Wuhan Institute of Physics and Mathematics, Chinese Academy of Sciences, Wuhan, China

Lijian Yang†
Department of Physics and Institute of Biophysics, Huazhong Normal University, Wuhan, China and Key Laboratory of Quark and Lepton Physics, Huazhong Normal University, Ministry of Education, Huazhong, People's Republic of China

(Received 22 January 2010; revised manuscript received 3 April 2010; published 28 June 2010)

When neurons in layer 1 fire irregularly under stochastic noise, it is found synchronous firings can develop gradually in latter layers within a feed-forward multilayer neural network, which is consistent with experimental findings. The underlying mechanism of propagation of firing rate is explored, then rate encoding realized by synchronization is clarified. Furthermore, the effects of connection probability between nearest layers, stochastic noise, and ratio of inhibitory connections to total connection on (i) propagation of firing rate by synchronization and (ii) coherence of firing pattern are investigated, respectively. It is observed that (i) there is a threshold for connection probability, beyond which firing rate of each layer can propagate successfully through the whole network by synchronization. The dependence of firing rate on layer index is very different for different connection probability. In addition, larger the connection probability is, more rapidly the synchrony is built up. (ii) Increasing intensity of stochastic noise enhances firing rate in output layer. Stochastic noise plays a constructive role in improving synchrony by causing the synchronization more quickly. (iii) The inhibitory connection offsets excitatory input therefore reduces firing rate and synchrony. As layer index increases, coherence measure goes through a peak, i.e., the coherence of firing pattern is the worst at certain a layer. With increasing the ratio of inhibitory connections, the variability of firing train is enhanced, exhibiting destructive role of inhibitory connections on coherence of firing pattern.

DOI: 10.1103/PhysRevE.81.061924 PACS number(s): 87.19.L−, 05.45.Xt

I. INTRODUCTION

Synchronization of neural activity appears in different parts of the mammalian cerebral cortex [1], and underlies different neural processes in both normal and anomalous brain functions [2]. It has been suggested that synchronization plays a vital role in information processing in the brain, e.g., processing information from different sensory systems to form a coherent and unified perception of the external world [1–9]. On the other hand, synchronization has been detected in pathological conditions such as Parkinson disease [10,11]. And epileptic seizures have long been considered resulting from excessive synchronized brain activity [12]. It has stimulated a great deal of theoretical and numerical works. By virtue of complex network methods, the effects of topological properties of underlying networks [13–16] are investigated. By using nonlinear dynamical analysis, many researches for synchronization mechanisms are also presented, such as dynamical properties of synaptic coupling [17,18], influence of efficacy of synaptic interaction on firing synchronization in excitatory neuronal networks [19], effects of distributed time delays on phase synchronization of bursting neurons [20], synchronization transition induced by synaptic delay in coupled fast-spiking neurons [21].

It is known that another research focus for neuron network is about the signal transmission and signal encoding. Neurons fire spikes when the total dendritic inputs reach a threshold, and information is encoded in the spike trains. There are two kinds of encoding mechanisms, namely, the firing rate and the spike timing. The firing-rate encoding is a traditional coding scheme, assuming that most, if not all, information about the stimulus is contained in the firing rate of the neuron. As the sequence of action potentials generated by a given stimulus varies from trial to trial, neuronal responses are typically treated statistically or probabilistically. They may be characterized by firing rates, rather than as specific spike sequences [22]. Differently, when precise spike timing or high-frequency firing-rate fluctuations are found to carry information, the neural code is often identified as a temporal code. A number of studies have found that the temporal resolution of the neural code is on a millisecond time scale, indicating that precise spike timing is a significant element in neural coding [23]. In nervous systems, information is transferred from one neuron group to its next groups [22], and many functional groups are involved in every informational processing.

Recently, it is found, theoretically and experimentally, the information encoding, especially firing-rate encoding, is tightly associated with synchronization process [24–27] in various neuronal networks. Among these networks, an interesting and well studied model is multilayer feed-forward network. It was found that synchronous firings can be propagated in a stable manner through such a network under appropriate conditions [24]. The firing rates of deep layers seem to be independent of the input firing rate in an

*Corresponding author; yiming@wipm.ac.cn
†lijian_yang@phy.ccnu.edu.cn

integrate-and-fire model [25]. Then propagation of the rate code in a feed-forward network was argued to be almost impossible [25]. However, this may be neuronal model dependent. To study the precise role of synchronous neuronal firing in signal encoding and examine what kinds of signals can be carried by synchrony [26,27], a multi layer feed-forward network of neurons in an *in vitro* slice preparation of rat cortex using an iterative procedure is reproduced. This experiment showed that when constant and time-varying frequency signals were delivered to the network, the firing of neurons in successive layers became progressively more synchronous. Notably, synchrony in the *in vitro* network developed even with uncorrelated input, persisted under a wide range of physiological conditions and was crucial for the stable propagation of rate signals. The firing rate was represented by a classical rate code in the initial layers, but switched to a synchrony-based code in the deeper layers, implying that synchrony plays an important role in the rate coding scheme. It will be interesting to provide a theoretical work to investigate the relation between synchronization and signal processing in neuron network.

In order to clarify how synchronization dynamics contribute to rate encoding, some theoretical questions remain unclear. (i) How to associate the experimental observations in Ref. [26] with a theoretical model. How the structure of neuron network determines its encoding function. (ii) What is the underlying mechanism leading to synchronization phenomena in the neuron network. By using a simple McCulloch-Pitts model, the research work by Nowotny has already shown that threshold function of neurons and feed-forward character of the network are sufficient to explain the observed synchronization phenomena [28]. No other detail of the neuron dynamics is necessary. While in our paper, the Hodgkin-Huxley (HH) neuron model is used because HH neurons model firings more realistically. In addition, our coupled HH neurons model provides rich parameters, which is advantageous to give some quantitative predictions for future experiments. Therefore, based on the potential neuron network structure with HH neuron model, it is possible to make further efforts to answer another two important questions as below. (iii) What is the effect of connection probability and stochastic noise on firing-rate propagation by synchronization. (iv) Most previous researches for rate encoding are focused on excitatory synapse, however inhibitory connection is also important [29]. Inhibitory synapses constitute approximately 15% of the synapses on cortical neurons. Most of these synapses arise from smooth stellate neurons within 400 microns of the target cell, but some are from basket cells as far as 1–1.5 mm away. Recurrent loops involving two or more neurons with excitatory and inhibitory synapses are found in biological systems such as hippocampus [30–32]. Therefore, the excitatory synapse and inhibitory synapse should be simultaneously considered. Few work has been referred to that so far.

To get an insight into the above questions, a theoretical model of ten-layer feed-forward multilayer network is provided. We show that firing rate can be propagated by synchronization in this feed-forward neuronal network. This is relevant to the propagation of the rate signal, consistent with experimental findings. This paper is organized as follows.

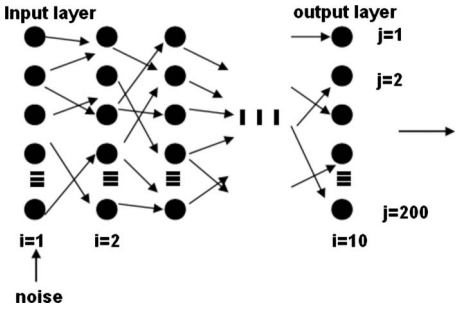

FIG. 1. A schematic of the model of a ten-layer feed-forward network with 200 neurons in each layer. Each neuron receives $200 \times P_1$ inputs from the previous layer. P_1 denotes the connection probability between nearest layer.

The feed-forward network model is introduced in Sec. II. In Sec. III, simulation results of the theoretical model show that synchronous firings can develop gradually within this network. Then the underlying mechanisms of propagation of firing rate realized by synchronization are clarified. Furthermore, the effects of connection probability between nearest layer, stochastic noise, and ratio of inhibitory connections to the total connection on (i) propagation of firing rate by synchronization and (ii) coherence of firing pattern are investigated, respectively. We end with our conclusions in Sec. IV.

II. MODELING AND SIMULATION

A ten-layer feed-forward network with $N=200$ HH neurons in each layer is constructed, as shown in Fig. 1. Layer 1 is called as input layer. Noise is introduced into the input layer only and causes the neurons in layer 1 to fire randomly. Each neuron in latter layers (i.e., layer 2,3,…,10) receives synaptic inputs randomly about $M=200 \times P_1$ from the previous layer, P_1 is the connection probability between any two adjacent layers. Layer 10 is considered as output layer. There are no couplings between the neurons within the same layer. The dynamical equations for the network are

$$C_m \frac{dV_{ij}}{dt} = -[g_{\mathrm{K}} n_{i,j}^3 (V_{ij} - V_{\mathrm{K}}) + g_{\mathrm{Na}} m_{i,j}^3 h_{i,j} (V_{ij} - V_{\mathrm{Na}}) + g_l (V_{ij} - V_l)] + I_0 + I_{i,j}^{syn}(t) + \xi_{1,j}(t), \quad (1)$$

where V_l is the resting leakage potential for a leakage conductance g_l, V_{K}, and V_{Na} are K^+ and Na^+ reversal potentials, C_m is the capacitance, where g_{Na}, g_{K}, and g_l are the maximum conductances for the sodium, potassium and leak currents. The membrane potential of neuron j in layer i is represented with V_{ij}. $m_{i,j}$ and $h_{i,j}$ are the activation and inactivation variables of the sodium current and $n_{i,j}$ is the activation variable of the potassium current. The gating variables $y_{i,j}=m_{i,j}$, $h_{i,j}$, $n_{i,j}$ satisfy the differential equation

$$\frac{dy_{i,j}(t)}{dt} = \alpha_y [1 - y_{i,j}(t)] - \beta_y y_{i,j}(t), \quad (2)$$

with nonlinear functions α_y and β_y given by

$$\alpha_m = 0.1(V+40)/\{1 - \exp[-(V+40)/10]\}, \quad (3)$$

$$\beta_m = 4\ \exp[-(V+65)/18], \tag{4}$$

$$\alpha_h = 0.07\ \exp[-(V+65)/20], \tag{5}$$

$$\beta_h = 1/\{1+\exp[-(V+35)/10]\}, \tag{6}$$

$$\alpha_n = 0.01(V+55)/\{1-\exp[-(V+55)/10]\}, \tag{7}$$

$$\beta_n = 0.125\ \exp[-(V+65)/80]. \tag{8}$$

For simplicity, the subscript ij for V_{ij} is neglected. The parameter values are $V_{\mathrm{Na}}=50$ mV, $V_{\mathrm{K}}=-77$ mV, $V_l=-54.4$ mV, $g_{\mathrm{Na}}=120$ mS/cm^2, $g_{\mathrm{K}}=36$ mS/cm^2, $g_l=0.3$ mS/cm^2, and $C_m=1$ μF/cm^2 [33–35]. The choice of parameters in Eqs. (3)–(8) is the same as that in the original paper written by Hodgkin and Huxley [33]. The original HH equations not only provide a good model for spike generation and conduction in the squid axon, but also incorporate the important features of neuronal excitability, activation and inactivation of voltage-dependent currents taking place at different time scales. The proper biophysical level of abstraction used by Hodgkin and Huxley enables direct experimental assessment of model parameters, as well as the natural extension of the model to more complicated excitable membranes than that of the squid giant axon.

I_0 is a constant injected current, and we set $I_0=1$ μA/cm^2 through paper. The Gaussian white noise satisfies $\langle \xi_{1,j}(t)\rangle=0$, $\langle \xi_{1,j}(t_1)\xi_{1,m}(t_2)\rangle=2D_1\delta_{j,m}\delta(t_1-t_2)$. D_1 is the noise intensity introduced in layer 1. It is noted the noise imposed on all neurons in layer 1 is the only input for the whole neuron network.

We adopt the synaptic current $I_{i,j}^{syn}(t)$ from layer (i-1) described by an alpha function [35]. The alpha function synapse is a phenomenological model based on an approximate correspondence of the time course of the waveform to physiological recordings of the postsynaptic response [36]. The equation of the synapse is like

$$I_{i,j}^{syn}(t) = -\frac{1}{M}\sum_{p=1}^{M} g_{syn}\alpha(t-t_{i-1,p})(V_{i,j}-V_{syn}), \tag{9}$$

with

$$\alpha(t) = (t/\tau)\exp(-t/\tau)\Theta(t). \tag{10}$$

Where τ is the characteristic time of the interaction, $\Theta(t)$ is the Heaviside step function, and $t_{i-1,p}$ is the beginning time of the synaptic interaction, i.e., the firing time of the presynaptic neuron pth in layer $(i-1)$ coupled with neuron (i,j). First, the synaptic inputs are all considered as excitatory (i.e., the cases investigated in Sec. III A and III B). So, we take $V_{syn}=0.0$ mV for excitatory synapses. Equation (10) yields pulses with the maximum value of e^{-1} at $t=t_{i-1,p}+\tau$ and with the half-width of 2.45τ [37]. So τ characterizes the duration of the synaptic interaction. τ is set to 2 ms and g_{syn} is fixed as 0.6 unless specified elsewhere.

Firings of each neuron are recorded and converted into a time series of standard pulses $U_j=U_A$ or U_B with $U_A=1$ of width 2 ms and $U_B=0$ corresponding to the firing and nonfiring states. For numerical integration of Eqs. (1) and (2), the Euler method is used with a time step of 0.001 ms. The additive Gaussian white noises in the Langevin equations, i.e., Eq. (1), are generated by Box-Mueller algorithm method [38].

III. RESULTS

A. Successful propagation of firing rate by synchronization

Now, as an illustration, the simulation results under the noise intensity $D_1=5.0$ and the connection probability $P_1=0.1$ are provided in Fig. 2. The firing patterns in different layers are plotted in Fig. 2(a). For each layer (e.g., layer 1,2,3,4,7,10), the post stimulus time histograms (PSTH) are shown in Fig. 2(b) accordingly. The PSTH shows the number of spikes collected at the output of the summing center per unite time. As a function of time, the PSTH is known as the instantaneous firing rate. It was assumed that this function encodes the information of the signal. The denser the row of dots is in Fig. 2(a), the more pronounced the peak at the corresponding time is in Fig. 2(b).

(i) Subject to Gaussian white noise, each neuron in layer 1 fires spikes irregularly. It is observed that the spatiotemporal firing pattern exhibits a uniform distribution. (ii) In layer 2 and layer 3, the numbers of spikes decrease, implying that the firing rate decreases. However, there is a tendency of synchrony, and several blurry columns of spikes appear in the firing pattern in layer 2. This becomes clear in layer 3 and 4 where there are several distinct columns of firings. The underlying mechanism can be observed from the small time window from the PSTH in layer 3 and layer 4 [referring to the dashed red box in Figs. 2(a) and 2(b)]. It is shown that weak spike train [see arrow marked with 1 in Fig. 2(c)] fails to propagation while strong one (see arrow marked with 2) can be propagated successfully. Therefore, weak spike trains are lost, and strong spike trains lead to some clear column. (iii) At layer 7, the synchrony is well established, meaning that all (or almost all) 200 neurons fire spikes about simultaneously. Globally, the successful propagation of firing rate originated from layer 1 by synchronization is realized. The synchrony is created gradually in the feed-forward neuron network by (i) integrating and strengthening the spiking inputs reached simultaneously in each layer, (ii) weakening and even preventing the transmission of sparse spiking inputs.

As proposed in Ref. [28], the probability distribution for number A_i of active neurons in layer i, i.e., $P(A_i=a_i)$ is obtained by theoretical derivation. The development of synchronization in the feed-forward neuron network can be observed clearly by evolution of $P(A_i=a_i)$ from layer to layer. Therefore, motivated by this idea, based on the simulation data obtained in Fig. 2(b), we also plot directly probability distribution for different layer corresponding to the case in Fig. 2, as shown in Fig. 3. It is found the initial probability distribution for number of active neurons in the input layer will quickly develop to a bimodal distribution with sharp peaks at 0 and N, which is very obvious since layer 6. The synchronized events are those when all neurons fire (right peak at N) and the probability of events with just a few active neurons is practically zero. Obviously, the asymptotic

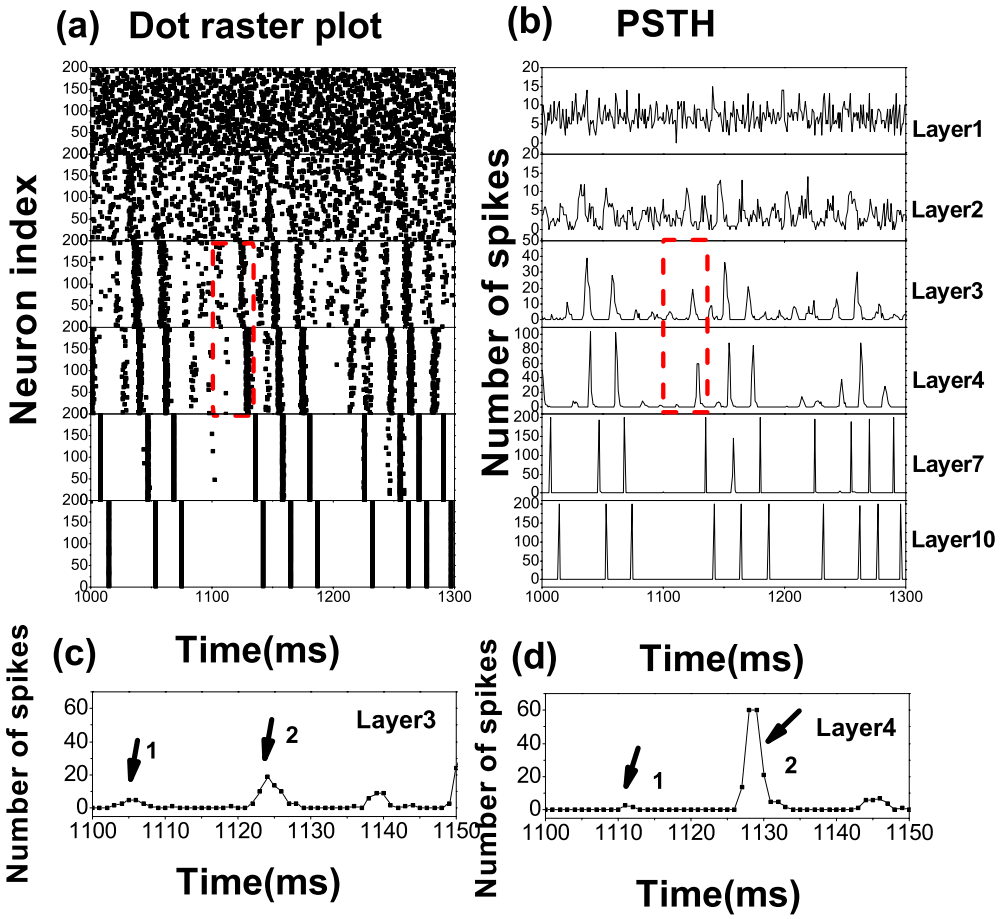

FIG. 2. (Color online) (a) Dot-raster plots of spike times of the network for $D_1=5.0$ and $P_1=0.1$ showing firing patterns in different layers. Each row of dots represents a spike train for a single neuron with index $1 \leq j \leq 200$. A synchrony means that all (or almost all) 200 neurons fire spikes about simultaneously. (b) The corresponding post stimulus time histograms (PSTH) showing the number of spikes collected at the output of the summing center per unite time. The denser the row of dots is in (a), more pronounced the peak at the corresponding time is in (b). (c) and (d) A small time window from the PSTH in layer 3 and layer 4 [referring to dashed red box in (a) and (b)] showing weak spike train (see arrow marked with 1) fails to propagation while strong one (see arrow marked with 2) can be propagated successfully.

bimodal distribution represents the synchronization phenomenon observed in Fig. 2.

An interesting question is raised about how the successful transmission of firing rate in the neuron network observed here originates from special network structure and neuron model. A detailed qualitative explanation about the dynamical mechanism is provided below. First, neurons in any given layer share a large quantity of common synaptic inputs. Here connection probability between neighboring layers is $P_1=0.1$, and neurons share about 1% of the same synaptic inputs, which leads to the correlation between the neurons. This common input tends to evoke spikes within a restricted time window, leading to partial synchrony between corresponding postsynaptic neurons. Second, for the HH neuron, most of postsynaptic currents do not actually contribute to the generation of spikes and only result in small fluctuations of membrane potential. Only coincident synaptic inputs can effectively trigger postsynaptic spikes, that is, the HH neuron is most sensitive to presynaptic pulses arriving simultaneously, acting as a detector for the temporal coincidence of presynaptic pulses.

In order to give a quantitative analysis for the signal transmission in the feed-forward neuron networks, furthermore, to clarify the relationship among network structure, dynamics and function, we investigate the effects of noise (D_1), connection probability (P_1) and ratio of inhibitory connections (P_2) on the propagation of firing rate by synchrony and the coherence of firing pattern below, respectively.

B. Effects of connection probability and stochastic noise on propagation of firing rate by synchronization

It is speculated that the successful propagation of firing rate produced in layer 1 may depend on the noise intensity D_1 and the connection probability P_1. If the noise intensity is small, the firings of spikes are quite sparse in layer 1, then the synchrony in later layers hardly occurs and the firing rate cannot be propagated in the network probably. This means a large enough noise intensity is required for the propagation of the rate signal. In addition, though it is enough for $P_1=0.1$, the connection probability cannot be too small, or else no enough common synapses are shared by neurons in the

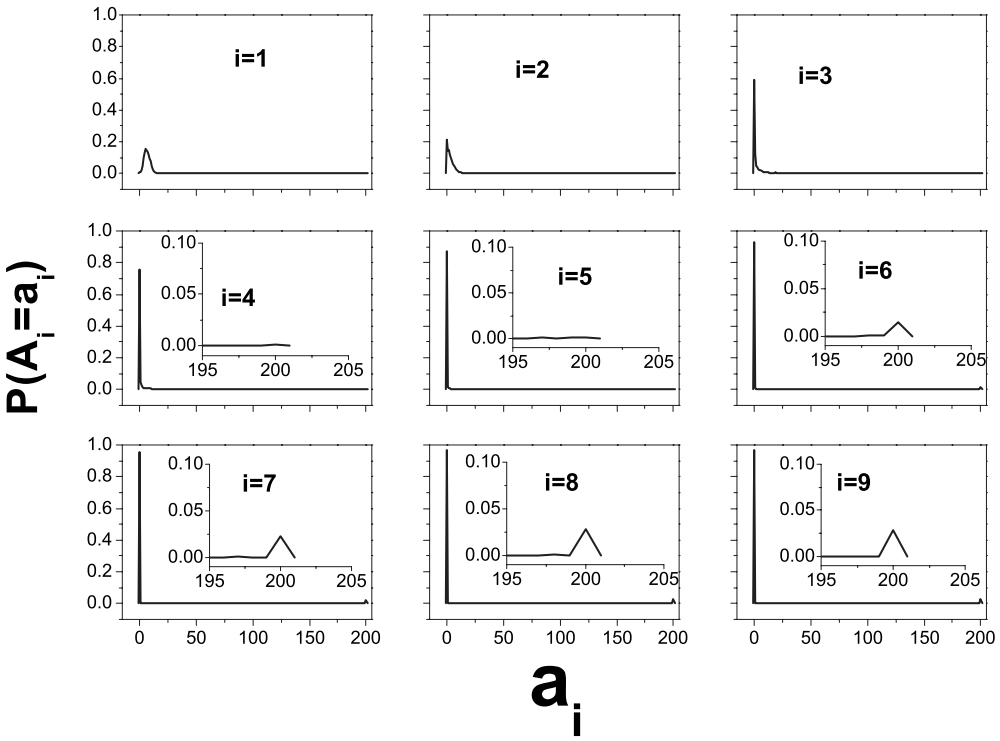

FIG. 3. The probability distribution for number A_i of active neurons in layer i corresponding to the case in Fig. 2. The insets show distribution around $a_i=N$, and this part of the distribution determines the probability of synchronous events.

same layer. In this subsection, a full investigation about the effect of connection probability and stochastic noise on propagation of firing rate by synchrony is provided.

Here we focus on two important aspects of the feed-forward neuron network: (i) the firing rate r_i in each layer, which is obtained by averaging over all the neurons in this layer within a long time window of 20 s, and (ii) synchrony of firing time of neurons K_i. We adopt the average cross correlation of firing time of neurons [39,40] to quantify the degree of firing synchronization. Average cross correlation is obtained by averaging the pair coherence $K_{i,jm}(\gamma)$ between neuron j and m, i.e.,

$$K_i = \frac{1}{N(N-1)} \sum_{j=1}^{N} \sum_{m=1, j\neq m}^{N} K_{i,jm}(\gamma). \tag{11}$$

The pair coherence $K_{i,jm}(\gamma)$ is defined as

$$K_{i,jm}(\gamma) = \frac{\sum_{l=1}^{k} X(l)Y(l)}{\left[\sum_{l=1}^{k} X(l) \sum_{l=1}^{k} Y(l)\right]^{1/2}}, \tag{12}$$

which is measured by the cross correlation of spike trains at zero time lag within a time bin γ. To transform the neuronal activity into spike train, the interval T_2-T_1 is divided into k bins of $\gamma=1$ ms. Then spike trains of neurons i and j are given by $X(l)=0$ or 1 and $Y(l)=0$ or 1 $(l=1,\ldots,k)$, where 1 represents a spike generates in the bin and 0 otherwise.

The firing rate and corresponding synchrony measure in each layer under different connection probability and different noise intensity are plotted in Fig. 4 and Fig. 5.

(i) When connection probability is very small, e.g., $P_1=0.05$, the same synaptic inputs shared by different neuron for each layer is small. It is observed that the signal of firing rate produced in layer 1 decays quickly even under the strong noise $D_1=50.0$ (see solid black curves in Fig. 4). Therefore, no synchrony is created (see solid black curves in Fig. 5).

(ii) When connection probability is slightly large, e.g., $P_1=0.1$, neurons share about 1 percent of the same synaptic inputs. It is found interestingly that the firing rate decreases in the first three layers, and then increases to a saturated

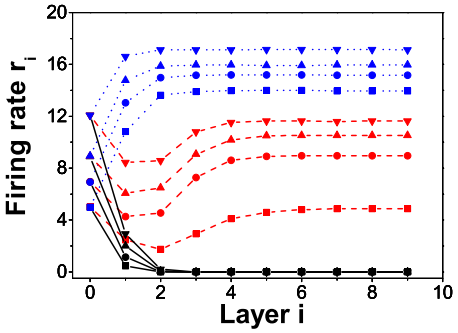

FIG. 4. (Color online) Firing rate r_i versus layer i for different noise intensities ($D_1=50.0$ (▼), $D_1=10.0$ (▲), $D_1=5.0$ (●), $D_1=3.0$ (■) and for different connection probability. Solid black lines:$P_1=0.05$. Dashed red lines:$P_1=0.1$. Dotted blue lines:$P_1=0.5$.

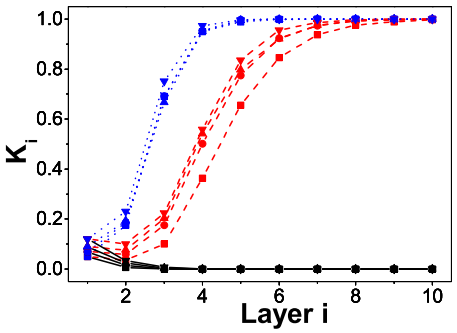

FIG. 5. (Color online) Synchrony measure K_i versus layer i for different noise intensities (D_1=50.0 (▼), D_1=10.0 (▲), D_1=5.0 (●), D_1=3.0 (■) and for different connection probability. Solid black lines:P_1=0.05. Dashed red lines:P_1=0.1. Dotted blue lines:P_1=0.5.

value (see dashed red curves in Fig. 4). Correspondingly, the synchrony becomes better with deeper layer and a full synchrony is already achieved in the layer 8 (see dashed red curves in Fig. 5). Therefore, there is a threshold for P_1 beyond which the firing rate of each layer can propagate successfully through the whole network. Some observations should be pointed out here. First, such a development of synchrony is really related to the experimental observation in Ref. [26] where neuronal firings in iteratively constructed networks *in vitro* are asynchronous for the first 2–3 layers but become progressively more synchronous in successive layers. Second, an explanation about the curves of firing rate (see dashed red curves in Fig. 4) is provided. From layer 1 to layer 2, the firing rate decreases because the numbers of filtered firings are quite large and the neuron can fire only when sufficient numbers of presynaptic pulses arrive simultaneously. Differently, from layer 3 to layer 10, the firing rate increases and is finally saturated to a value since the synchronous firings can be propagated stably and the sparse firings almost disappear. Third, for each noise intensity, the firing rate in output layer (i.e., layer 10) nearly equals to that in input layer (i.e., layer 1), which implies a perfect rate encoding realized in the feed-forward multilayer neuron network.

(iii) When connection probability is very large, e.g., P_1 =0.5, the same synaptic inputs shared by different neuron is also very large. Interestingly, the dependence of firing rate on layer index is very different from that under P_1=0.1. A monotonous increasing curve of firing rate is observed (see dotted blue curves in Fig. 4), and firing rate is quickly saturated to a large value from layer 2. The full synchronization is achieved since layer 4 (see dotted blue curves in Fig. 5) with a better signaling efficiency than that for P_1=0.1. Therefore, larger the connection probability is, more rapidly the synchrony is built up.

Stochastic noise is unavoidable in real neuron network, how the noise affects the signal transmission and information encoding is also one focus of our research. By analysis of Fig. 4 and 5, some important results are observed: (i) Increasing the intensity of stochastic noise enhances the firing rate in output layer (i.e., the saturated value), which implies the output becomes stronger. (ii) Stochastic noise plays a constructive role in improving the synchrony by causing the

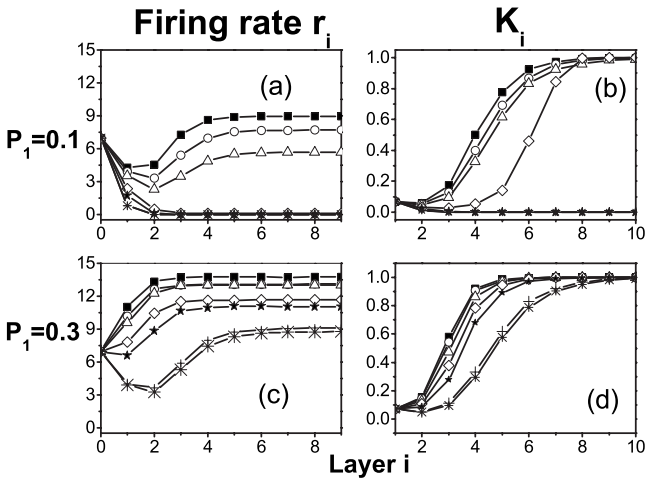

FIG. 6. Firing rate r_i (a) and (c) and synchrony measure K_i (b) and (d) for different ratio of inhibitory connections (P_2=0.5 (+), P_2=0.4 (∗), P_2=0.3 (⋆), P_2=0.2 (◇), P_2=0.1 (△), P_2=0.05 (○), P_2=0.0 (■)) when D_1=5.0. From top to bottom: P_1=0.1, P_1=0.3.

synchronization more quickly and the synchrony curve sharper. Hence stochastic noise increases the efficiency of synchrony in the feed-forward neural network, leading to a better synchronization. (iii) In addition, changing noise has bigger effects on firing-rate curve than that on synchrony curve. The sensitivity of r_i to stochastic noise is larger than that of K_i to noise.

C. Effects of ratio of inhibitory connections on propagation of firing rate and coherence of firing pattern

Above, the synaptic inputs are all considered as excitatory. However, inhibitory connection is also important, as introduced in Sec. I. The synaptic effect is traditionally classified as excitatory or inhibitory depending on the value of V_{syn}. Here, we take V_{syn}=0.0 mV for excitatory synapses, and −80 mV for inhibitory ones. In this subsection, the effects of the ratio of inhibitory connection to the total connection P_2 on propagation of firing rate and coherence of firing pattern are studied, respectively. P_2 means that the number of inhibitory synapses received in layer i from the layer $i-1$ is $200\times P_1\times P_2$, others are excitatory synapses. In addition, here we use the same time constant for the inhibitory connections as the one used for the excitatory connections (referring to the similar treatment in Ref. [25]).

First, we focus our attention on the effects of P_2 on propagation of firing rate and the results are shown in Fig. 6.

(i) For a weak connection probability, e.g., P_1=0.1 as shown in Figs. 6(a) and 6(b), it is observed that when the ratio of inhibitory connection is small [see the top three curves in Fig. 6(a)], with the increase of layer index, the firing rate is reduced first and then enhanced until the firing rate is saturated. It implies the firing rate is propagated successfully through the neuron network. Meanwhile, the synchronization among neuron in each layer is improved, and full synchronization is almost achieved since layer 6 [see the top three curves in Fig. 6(b)]. However, when the ratio of inhibitory connection is large [see the bottom three curves in

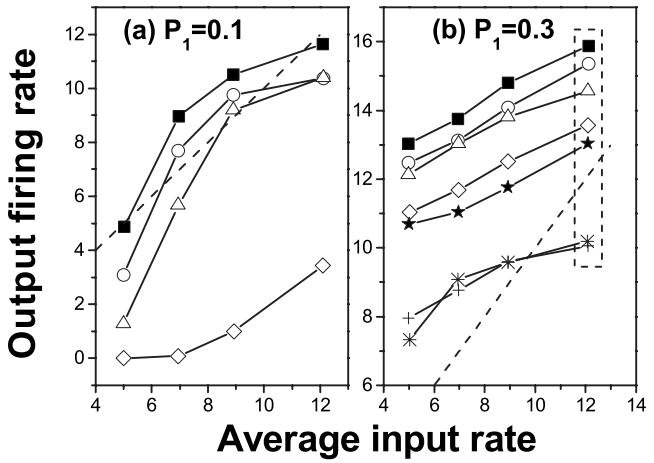

FIG. 7. Input-output relations for (a) $P_1=0.1$ and (b) $P_1=0.3$ under different ratio of inhibitory connections P_2. The inhibitory ratios P_2 have the same symbols as indicated in Fig. 6. The dashed lines give a reference curve with a slope of unity.

Fig. 6(a)], with the increase of layer index, the propagation of firing rate fails. Correspondingly, the synchronization among neuron in each layer is reduced quickly [see the bottom two curves in Fig. 6(b)]. A special case i.e., $P_2=0.2$(◇), is found. Though the firing rate is very small for $P_2=0.2$, the synchronization is still slowly achieved in layer 8. In sum, for weak connection probability, the inhibitory connection offsets the excitatory input, therefore reduces the firing rate. At the same time, increasing ratio of inhibitory connection destroys the propagation of firing rate, even makes the synchronization disappear completely.

(ii) For a strong connection probability, e.g., $P_1=0.3$ as shown in Figs. 6(c) and 6(d), it is found the propagation of firing rate by synchronization is also weakened due to raising P_2. However the firing rate which fails to propagate because of large P_2 in Fig. 6(a) [see the bottom two curves in Fig. 6(b)] (+,∗) now is supported and propagated successfully even the excitatory connection is balanced by inhibitory connection, i.e., the ratio of inhibitory connection $P_2=0.5$.

Furthermore, the effects of rate encoding are clarified. A plot of input-output relations is presented for different cases under which the synchronous firing is developed successfully, as shown in Fig. 7. The input rate is average value of firing rate produced in layer 1 under different noise intensity. Four average input rates, 5.0, 7.0, 9.0, and 12.0 in Fig. 7 are determined by four different noise intensities, $D_1=3.0$, $D_1=5.0$, $D_1=10.0$, and $D_1=50.0$, respectively. The output firing rate is derived from the firing rate in layer 10. It is found that though the input-output curves deviate from a linear curve with a slope of unity, the input and output firing rates are nearly same under some conditions. For example (i) for $P_1=0.1$, when the ratio of inhibitory connections P_2 is small, the deviation of input-output curve from the dashed line is also small. Especially, a good case for rate encoding (shown with dashed red lines in Fig. 4) can be observed clearer in Fig. 7 [see the top curve in Fig. 7(a)]. (ii) When $P_1=0.3$, our simulation data shows large average input rate, i.e., large noise intensity, is advantageous to a perfect rate encoding. Some points with large average input rates about 12.0 under $D_1=50.0$ are enclosed by a dashed box in Fig. 7(b). It is found the output firing rate, changed in a small relatively range from 10.0 to 16.0, is very close to the average input rate. It means this rate encoding is robust relatively to the change of ratio of inhibitory connections under large noise intensity.

Second, the effects of ratio of inhibitory connection P_2 on the coherence of firing pattern, are also investigated. A measure of coherence in layer i is provided by coefficient of variation R_i, which is derived as below

$$R_i = \frac{\sum_{j=1}^{N} (R_{ij})}{N}, \tag{13}$$

with

$$R_{ij} = \frac{\sqrt{\langle T_{ij}^2 \rangle - \langle T_{ij} \rangle^2}}{\langle T_{ij} \rangle}. \tag{14}$$

T_{ij} is the time interval of interspike in the firing of neuron j in layer i. The R_i actually measures spike train variability in layer i. It is obvious that higher the R is, weaker the coherence is, hence larger the variability of firing pattern is. Figure 8 shows the coherence measure R_i versus the layer index for different P_2.

(i) For a weak connection probability, e.g., $P_1=0.1$ [Fig. 8(a)], as the layer index increases, each R curve undergoes a maximum at certain a layer. It implies that the coherence of firing pattern is the worst at the peak of R curve. After the synchronization is achieved slowly from about layer 5, the R curve begins to drop down so that R is small, showing the coherence of firing pattern becomes better due to the occurrence of strong synchrony. At last the coherence is almost unchanged become of the stable synchronization.

Interestingly, with increasing ratio of inhibitory connections, the height of R curve rises until $P_2=0.1$, exhibiting the destructive role of inhibitory connections on the coherence of firing pattern. Furthermore, due to the failure of propagation of firing rate [Fig. 6(a)], the R curve for $P_2=0.2$ or larger P_2 drops down.

(ii) For a strong connection probability, e.g., $P_1=0.3$ [Fig. 8(b)], similar to the above case, the R in latter layers is small, hence the coherence of firing pattern in latter layer is enhanced and better than that in input layer due to the stronger synchrony. The height of peak for R curve is increased due to increasing P_2. It means that increasing ratio of inhibition connections leads to larger variability of firing pattern, the destructive role of inhibition connections on the coherence of firing pattern is very clear. It is noted that, in the case of balance between the excitatory and inhibitory connection for $P_2=0.5$, the variability of output spike train is the largest, i.e., the coherence is the worst. In addition, different with the case of $P_1=0.1$, even for $P_2=0.2$ or larger P_2, the curve does not descend because of successful propagation of firing rate

under $P_1=0.3$ [Fig. 6(c)]. Of course, comparing the R curves for same P_2 in (a) and (b), the R curve under $P_1=0.3$ is lower than that under $P_1=0.1$, showing the constructive role of connection probability on the coherence of firing pattern, which can be accepted qualitatively.

IV. DISCUSSIONS AND CONCLUSIONS

The transmission of information in neural network is an important topic in neuron science. Especially, it is interesting to provide a theoretical frame to investigate the relation between synchronization and rate encoding in neuron network. In this article, we construct a feed-forward multilayer neural network, it is found synchronous firings can develop gradually within our network, which is consistent with experimental findings in Ref. [26]. The underlying mechanism of propagation of firing rate is clarified, then the rate encoding realized by synchronization is illustrated. Furthermore, the effects of connection probability between nearest layers P_1, stochastic noise D_1, and the ratio of inhibitory connections to the total connection P_2 on (i) rate encoding by synchronization and (ii) coherence of firing pattern in such neuron network are investigated, respectively.

There is a threshold for P_1, beyond which firing rate of each layer can propagate successfully through the whole network. Accompanied by the propagation of firing rate, synchronization among neurons in the same layer occurs. The dependence of firing rate on layer index is very different for different connection probability (see Fig. 4). For example, if the connection probability is very small, e.g., $P_1=0.05$, the dependence of firing rate on layer index is a monotonous decreasing curve. While the firing rate decreases in the first three layers, and then increases to a saturated value when $P_1=0.1$. Furthermore, a monotonous increasing curve for firing rate is observed for $P_1=0.5$. In addition, larger the connection probability is, more rapidly the synchrony is built up (see Fig. 5).

Increasing the intensity of stochastic noise D_1 enhances firing rate in output layer. Stochastic noise plays a constructive role in improving the synchrony by causing synchronization more quickly and synchrony curve sharper, hence increases the efficiency of synchrony in the feed-forward neural network, leading to a better synchronization. In addition, the changing noise has bigger effects on firing-rate curve than that on synchrony curve.

When the inhibitory connection is considered, it offsets excitatory input therefore reduces firing rate and synchrony. As layer index increases, the R of firing trains goes through a peak, showing the coherence is the worst at a certain layer. With increasing P_2, the height of R curve rises, exhibiting destructive role of inhibitory connections on the coherence of firing pattern. It is noted that, in the case of balance between the excitatory and inhibitory connection, i.e., $P_2=0.5$ in Fig. 8(b), the variability of output spike train is the largest. Theoretical research in Ref. [25] has shown a balance between excitation and inhibition in a feed-forward network can account for randomness of firing time. Interestingly, by the investigation for coherence of firing pattern, our simulation result just provides a quantitative description for the randomness of firing time in a certain extent for the case of $P_2=0.5$.

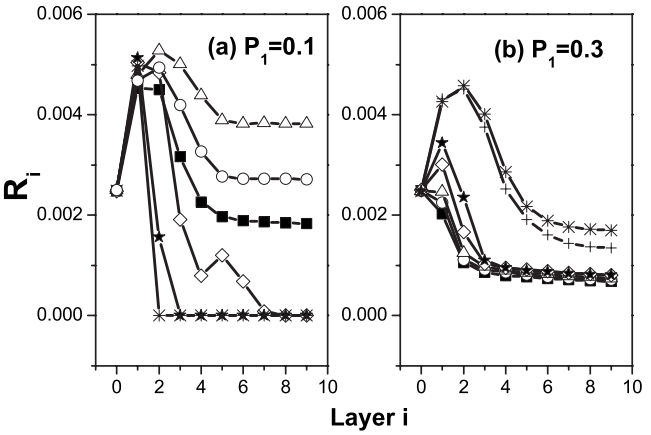

FIG. 8. Coherence measure R_i versus layer index i for different ratio of inhibition connections [$P_2=0.5$ (+), $P_2=0.4$ (∗), $P_2=0.3$ (⋆), $P_2=0.2$ (◇), $P_2=0.1$ (△), $P_2=0.05$ (○), $P_2=0.0$ (■)] when $D_1=5.0$. From left to right: $P_1=0.1$, $P_1=0.3$.

Theoretical work in Ref. [28] has already provided a very good explanation for the generality of synchronization developed in a feed-forward neuron network. Therefore, our theoretical model is only a specific example and just verifies the generality of the synchronization predicted by Nowotny. Especially the probability theory is used to derive theoretically the probability distribution for number of active neurons in each layer, hence the appearance or disappearance of synchronization is explored by probability distribution in Ref. [28]. This theoretical method is very significant and novel, which has stimulated further development of research for neuronal network dynamics. Motivated by this idea, as the first step, a simple investigation for the probability distribution of neuron firing is also provided in this paper (see Fig. 3). It should be pointed out that the biological background of HH neuron model is stronger, therefore, our coupled HH neuron model is appropriate for the further extension to consider more biological complexities. In addition, the rich parameters in this theoretical model provide us plenty of control variables, therefore a full investigation, such as the effects of P_1, P_2, and D_1 on neuron network dynamics, including synchronization of firing pattern and coherence of firing trains, can be given theoretically. The signification of our work just lies on such a full quantitative investigation.

Some problems deserve our close attention. In our model, the internal connection among neurons in the same layer and the possible feedback in different layer are both not considered. Based on the further experimental findings about the neural network structure, it is necessary to improve our model. The stochastic noise is only introduced into layer 1 in order to create the signal input of firing rate, we will investigate the case when all the neurons are disturbed by noise in future. In addition, for real neural network, how to determine the connection probability and the ratio of inhibitory connection, and whether these control parameters are variable are both challenging tasks, which are our next focuses. Our research provides a theoretical frame to correlate the

synchronization dynamics with signal encoding in neuron network, and gives a clear investigation about the relationship between the structure (e.g., connection probability between nearest layers, and the ratio of the inhibitory connections) and function (e.g., rate encoding and coherence of firing pattern) of neuron network.

ACKNOWLEDGMENT

This work was supported by the National Natural Science Foundation of China under Grant No.10905089 (M.Y.), TianYuan Special Funds under Grant No.10926065 (M.Y.), Key Laboratory of Quark & Lepton Physics (Huazhong Normal University) QLPL200905 (L.J.Y.).

[1] W. Singer and C. M. Gray, Annu. Rev. Neurosci. **18**, 555 (1995).
[2] A. K. Engel, P. Fries, and W. Singer, Nat. Rev. Neurosci. **2**, 704 (2001).
[3] C. von der Malsburg, Neuron **24**, 95 (1999).
[4] A. Roskies, Neuron **24**, 7 (1999).
[5] W. Singer, Neuron **24**, 49 (1999).
[6] M. I. Rabinovich, P. Varona, A. I. Selverston, and H. D. I. Abarbanel, Rev. Mod. Phys. **78**, 1213 (2006).
[7] M. Dhamala, V. K. Jirsa, and M. Ding, Phys. Rev. Lett. **92**, 074104 (2004).
[8] S. L. Bressler, R. Coppola, and R. Nakamura, Nature (London) **366**, 153 (1993).
[9] M. Joliot, U. Ribary, and R. Llinas, Proc. Natl. Acad. Sci. U.S.A. **91**, 11748 (1994).
[10] A. Nini, A. Feingold, H. Slovin, and H. Bergman, J. Neurophysiol. **74**, 1800 (1995).
[11] C. Hammond, H. Bergman, and P. Brown, Trends Neurosci. **30**, 357 (2007).
[12] R. K. Wong, R. D. Traub, and R. Miles, Adv. Neurol. **44**, 583 (1986).
[13] L. F. Lago-Fernández, R. Huerta, F. Corbacho, and J. A. Sigüenza, Phys. Rev. Lett. **84**, 2758 (2000).
[14] B. Percha, R. Dzakpasu, M. Zochowski, and J. Parent, Phys. Rev. E **72**, 031909 (2005).
[15] S. Feldt, H. Osterhage, F. Mormann, K. Lehnertz, and M. Żochowski, Phys. Rev. E **76**, 021920 (2007).
[16] D. H. Zanette and A. S. Mikhailov, Phys. Rev. E **58**, 872 (1998); Q. Li, Y. Chen, and Y. H. Wang, *ibid.* **65**, 041916 (2002); S. J. Wang, X. J. Xu, Z. X. Wu, and Y. H. Wang, *ibid.* **74**, 041915 (2006).
[17] H. Sakaguchi, Phys. Rev. E **73**, 031907 (2006).
[18] R. Zillmer, R. Livi, A. Politi, and A. Torcini, Phys. Rev. E **74**, 036203 (2006).
[19] S. J. Wang, X. J. Xu, Z. X. Wu, Z. G. Huang, and Y. H. Wang, Phys. Rev. E **78**, 061906 (2008).
[20] X. M. Liang, M. Tang, M. Dhamala, and Z. H. Liu, Phys. Rev. E **80**, 066202 (2009).
[21] Q. Y. Wang, Q. S. Lu, and G. R. Chen, Int. J. Bifurcation Chaos Appl. Sci. Eng. **4**, 1189 (2008).
[22] F. Rieke *et al.*, *Spikes Exploring the Neural Code* (MIT Press, Cambridge, MA, 1997).
[23] J. J. Hopfield, Nature (London) **376**, 33 (1995).
[24] M. Diesmann, M.-O. Gewaltig, and A. Aertsen, Nature (London) **402**, 529 (1999).
[25] V. Litvak, H. Sompolinsky, I. Segev, and M. Abeles, J. Neurosci. **23**, 3006 (2003).
[26] A. D. Reyes, Nat. Neurosci. **6**, 593 (2003).
[27] I. Segev, Nat. Neurosci. **6**, 543 (2003).
[28] T. Nowotny and R. Huerta, Biol. Cybern. **89**, 237 (2003).
[29] Michael N. Shadlen, William T. Newsome, Curr. Opin. Neurobiol. **4**, 569 (1994).
[30] T. F. Freud and G. Buzsaki, Hippocampus **6**, 345 (1996).
[31] Z. F. Kisvárday, C. Beaulieu, and U. T. Eysel, J. Comp. Neurol. **327**, 398 (1993).
[32] M. von Krosigk, T. Bal and D. A. McCormick, Science **261**, 361 (1993).
[33] A. L. Hodgkin and A. F. Huxley, J. Gen. Physiol. **117**, 500 (1952).
[34] W. Gerstner and W. M. Kistler, *Spiking Neuron Models: Single Neurons, Populations, Plasticity* (Cambridge University Press, Cambridge, England, 2002).
[35] D. Hansel, G. Mato, and C. Meunier, EPL **23**, 367 (1993).
[36] A. Destexhe, Z. F. Mainen, and T. J. Sejnowski, Neural Comput. **6**, 14 (1994).
[37] H. Hasegawa, Phys. Rev. E **61**, 718 (2000).
[38] R. F. Fox, I. R. Gatland, R. Roy, and G. Vemuri, Phys. Rev. A **38**, 5938 (1988).
[39] X. J. Wang and G. Buzsaki, J. Neurosci. **16**, 6402 (1996).
[40] S. Wang, W. Wang, and F. Liu, Phys. Rev. Lett. **96**, 018103 (2006).